

We are IntechOpen, the world's leading publisher of Open Access books Built by scientists, for scientists

6,900

Open access books available

186,000

International authors and editors

200M

Downloads

Our authors are among the

154

Countries delivered to

TOP 1%

most cited scientists

12.2%

Contributors from top 500 universities



WEB OF SCIENCE™

Selection of our books indexed in the Book Citation Index
in Web of Science™ Core Collection (BKCI)

Interested in publishing with us?
Contact book.department@intechopen.com

Numbers displayed above are based on latest data collected.
For more information visit www.intechopen.com



Current Transducer for IoT Applications

Erik Leandro Bonaldi, Levy Ely de Lacerda de Oliveira, Germano Lambert-Torres, Luiz Eduardo Borges da Silva and Vitor Almeida Bernardes

Abstract

The evolution of communication technology and the reduction of its costs have driven several advances in measurement systems. Points that could not be measured before can now be monitored. Points with difficulty to reach or with major security restrictions can begin to have their quantities measured and informed to control centers. This chapter presents one of these evolutions showing a current transducer (CT), which can measure this magnitude, make an initial treatment of the signal, and transmit it to a panel or control center. Besides, this current transducer does not require an energy source to operate, being self-powered by the current it is measuring. Because it is inexpensive, it can be spread through the facilities, supplying the current at various points of the observed electrical network. With signal treatment, useful information can be inserted in this device so that it informs already preprocessed elements to reading devices, becoming part of the world of IoT. This article presents its use in motor condition monitoring at the Pimental hydroelectric power plant.

Keywords: measurement, current transducer, IoT, IIoT, energy monitoring, condition-based maintenance

1. Introduction

In recent times, new scenarios, many of them futuristic and revolutionary, have emerged based on technological advances in two areas, the development of processors with high processing power and high energy efficiency [1] and the development of communication protocols with high transfer rates and low consumption [2].

On the one hand, these advances have stimulated a revolution in the world of sensors that has been called the “Industrial Internet of Things” (IIOT) [3–5], where it is seen that all devices will present, shortly, some kind of intelligence and interconnection through the Internet. On the other hand, in the industrial environment, another revolution related to these technological advances has been establishing, the so-called fourth Industrial Revolution, or Industry 4.0 [6, 7], where the physical systems of the factory floor will have their parameters monitored and digital models of your operative and maintenance condition will be updated for decision-making and optimization purposes.

And more, another equally strong trend, due to concerns about the environmental impact generated by all this diffusion of consumer electronics and industrial electronics, is the energy collection from the environment, named “energy

harvesting.” This tendency is based on the energy collection from the environment to drive highly efficient electronics, avoiding the dependence of the electrical system and eliminating the use of batteries or significantly reducing it. Another advantageous aspect of devices with power collection is related to the ease of installation, since power sources and cables connected to power outlets are not required, configuring a wireless power supply.

In accordance with those recent trends, this chapter proposes a wireless self-supplied current transducer (CT) as an IIOT application for induction motor monitoring. Section 2 presents an overview of the proposed current transducer and the modeling considerations about the measurement and power extraction CTs. In Section 3, the basic components used in the implementation of the proposed current transducer are presented. Section 4 considers the available wireless interface standards and details the chosen one. The final assembly of the resulting prototype is presented in Section 5. In Section 6, test results are presented attesting the prototype performance. And Section 7 presents the conclusions.

2. Overview of the current transducer

Figure 1 presents the general overview of the developed current transducer, where there are two current transducers, one for measurement and the other for energy extraction. The system is complete with a wireless communication module, IEEE 802.11 Standard (Wi-Fi) [8]. The device presented in this chapter can be applied widely throughout the industrial sector, regardless of its specificity, since the need of current measurement for energy monitoring or monitoring of the condition of machinery is widespread enough.

2.1 Measuring CT modeling

For monitoring large-scale equipment, the measurement units can be considered ideal transformers in the frequency range of interest between ~ 5 and ~ 3 kHz. The only concern is the input impedance of the AD converter which is in parallel with the “shunt” resistor in a direct connection or the input impedance of the amplifier making the buffer function to protect the AD converter in an indirect connection. However, in both cases, the input impedance tends to be much higher than 50Ω . For a direct connection to the AD converter, the input impedance for the high-resolution mode is $16.4 \text{ k}\Omega$. For a connection through a buffer, for example, the suggested configuration on the ADS1271EVM rating board, the 50Ω shunt will

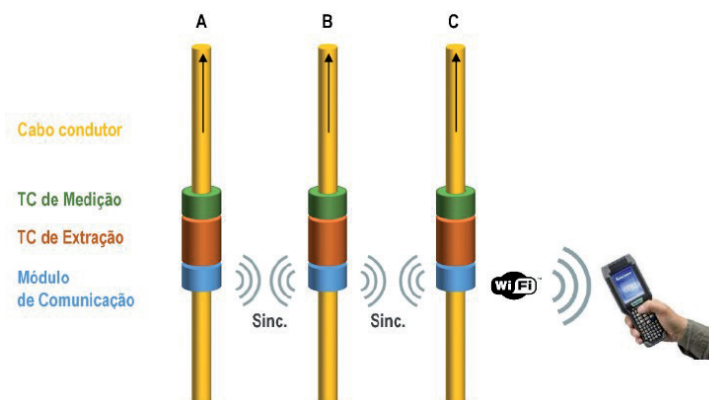


Figure 1.
Concept of application of the wireless and self-powered current transducer.

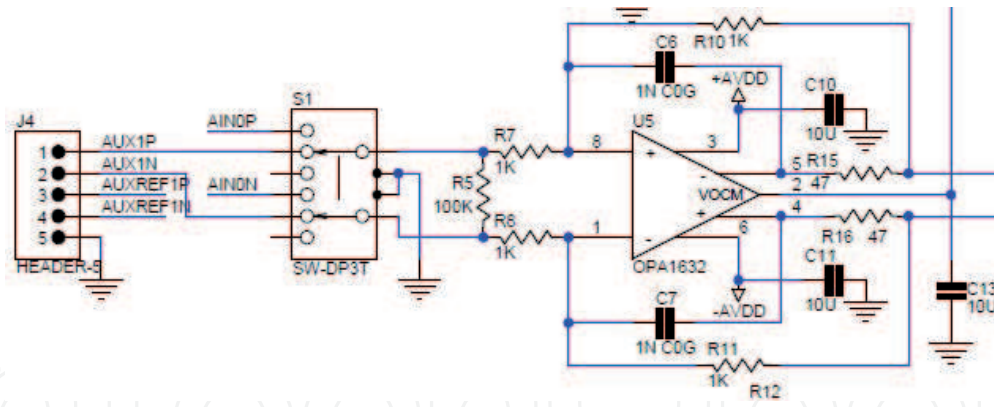


Figure 2.
 ADS1271EVM evaluation board input buffer.

be in parallel with the 100 kΩ/2 kΩ arrangement which is about 40 times greater. **Figure 2** presents this arrangement. There are arrangements with a better input impedance, but it is worth remembering that any minor transformation relationship errors arising from the interaction between shunt resistor and input impedance can be compensated by a software in the microcontroller.

2.2 Modeling and simulation of the power extraction CT

An extraction CT can be modeled by the scheme and equation shown in **Figure 3**. As can be perceived, the power in the load, R_L , depends on the current in the secondary of the CT, I_s , and the current splitter formed by the inductance of magnetization, L_m , and the own load, R_L . The higher the L_m , the higher is the portion of the current of the secondary that will pass through the load, I_L , and the higher is the power extracted.

In **Figure 3**, by the equation of the magnetization inductance referred to the secondary, $L_{m,s}$, it is perceived that it is proportional to the effective area of its section, A_e , and is inversely proportional to its average length, D . On the other hand, the magnetization inductance is also proportional to the square of the number of turns of the secondary, N_2 . However, the increase in N causes the decrease of the current of the secondary and therefore of the power in the load so that there is an optimum value of N for a given configuration. For modeling, a common CT with a bipartite

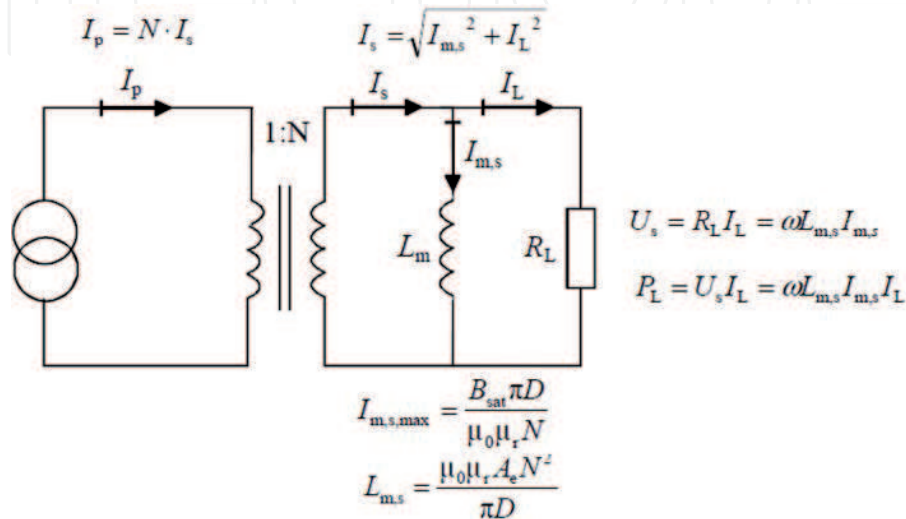


Figure 3.
 CT modeling of power extraction, schematic, and equations (toroidal core).

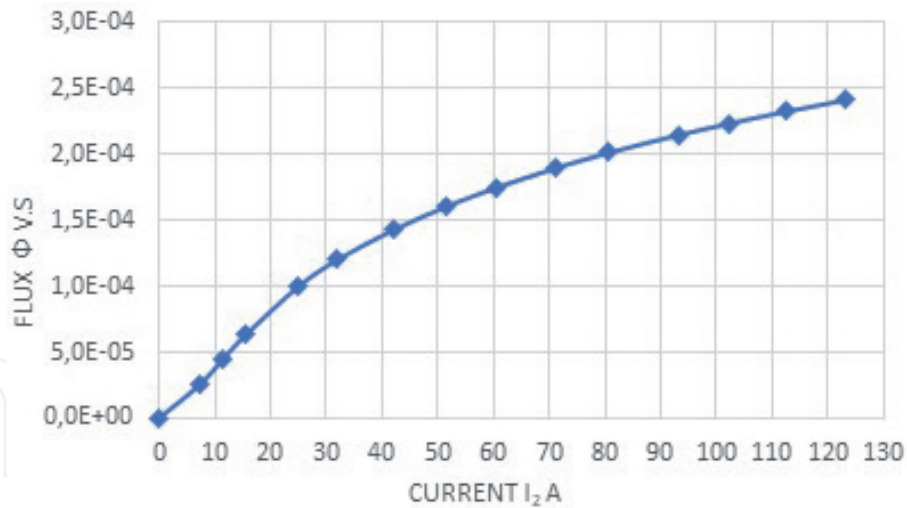


Figure 4.
CT magnetization curve.

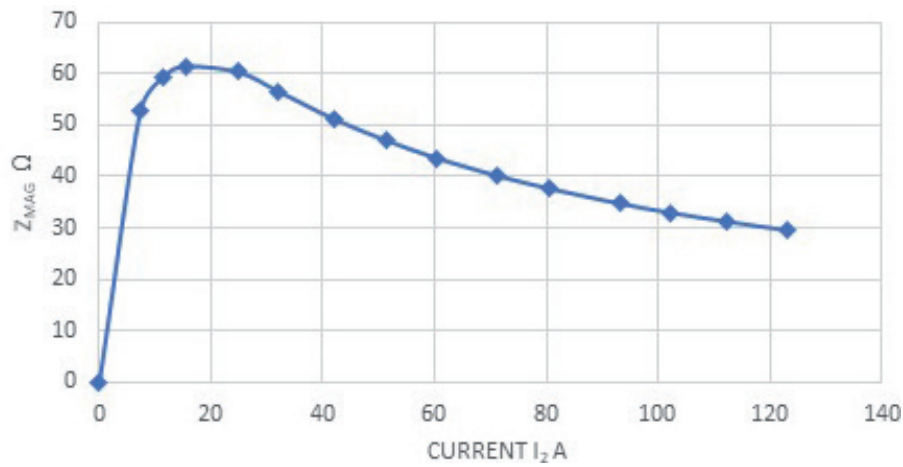


Figure 5.
Behavior of CT magnetization impedance.

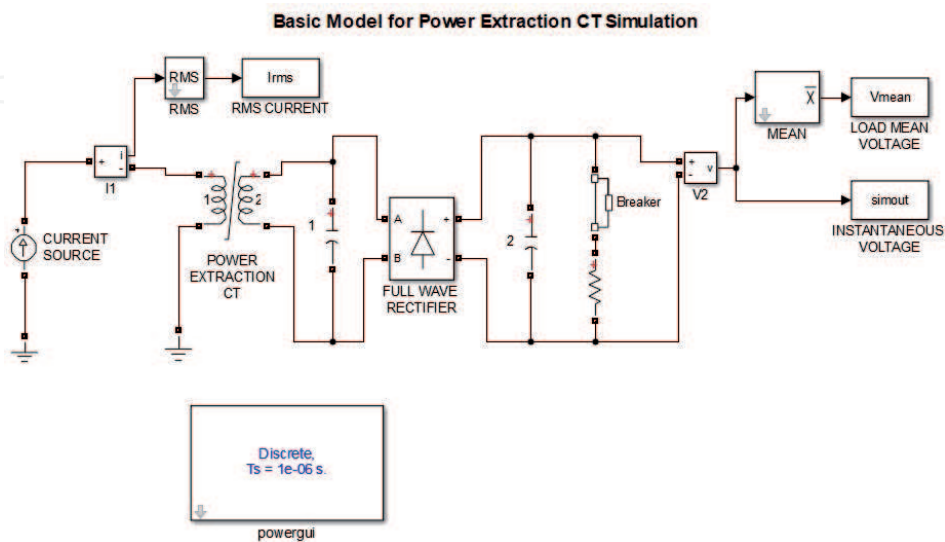


Figure 6.
Model for computational simulation.

silicon steel core is used, presenting an original transformation ratio of 250A:1A, a mass of 411 g (including the original winding), and a nominal area of 128 mm².

Figure 4 presents the magnetization curve of the core, separately and together. The tendency of CT with double core saturated with a higher current in the primary is perceived. In any case, according to the estimated currents and measurements in the cable, the CT works far from the core saturation point. It should also be noted that the saturation of the core plays an important role in the aid to the protection of the extractor electronics. **Figure 5** presents the behavior of the magnetization impedance of the test core.

Figure 6 presents the model for computational simulation of the power extraction CT. The transformer block uses the magnetization curve shown above. In this model a CT self-inductance compensation capacitor, a complete wave rectifier to produce a continuous voltage in the load, and a capacitor for voltage “ripple” filtration are included. The resistor has been chosen to be equivalent to the load of the application. It was estimated, previously, that the final prototype would be equivalent to a maximum load of 1.1 W, operating at 5 VDC. This power equates to a resistive load of 22.72 Ω , which was approximated to a load of 25 Ω , for availability, with three 75 Ω resistors in parallel being used.

3. Implementation of the current measurement module

The current measuring module digitalizes the output of the measuring CT and makes it available for processing and transmission. The digital-to-analog conversion is performed by the ADS1271 converter, and its control is performed by the CC3200 microcontroller. The interconnection of the two modules, ADS1271 and CC3200, is presented in the figure below. The set is powered by 5 VDC, and communication between modules is done by the serial peripheral interface (SPI) communication interface.

The CC3200 microcontroller is the master device, and the ADS1271 is the slave device in the SPI communication scheme. The master device provides the clock signal for the SPI interface of the slave device, which sends the data signal (PIN slave out-master in) to the master device. The slave device also sends the data-ready signal to an interrupt line of the master device, interrupting the microcontroller and stating that a valid data is ready for reading and processing.

The power metering module is composed of the magnetic field power extraction CT and the power conditioning circuit. The extraction CT is composed of the core and the winding of the secondary, whose main parameter is the number of turns, which is determined, to extract the estimated power for the application with the minimum current in the primary.

The power conditioning circuit consists of compensating capacitors, a full-wave rectifying bridge, and a DC-DC converter with buck topology, whose main parameter is the output voltage, defined by the power supply voltage of the electronics of the application, in this case 5 VDC. In the buck topology, the output voltage is

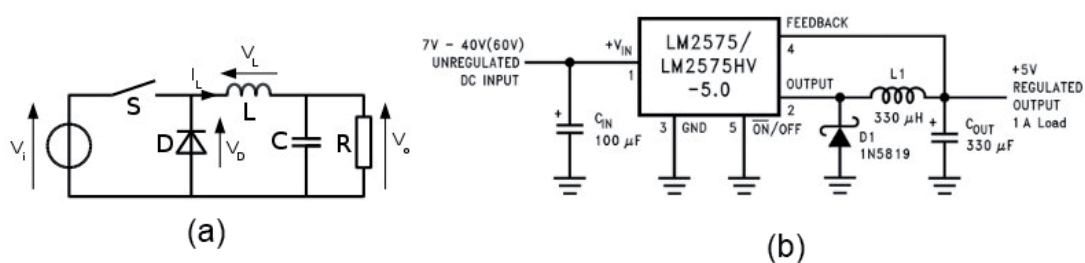


Figure 7. DC-CC converter with buck topology: (a) overall topology scheme and (b) real circuit with integrated circuit LM2575-5.0.

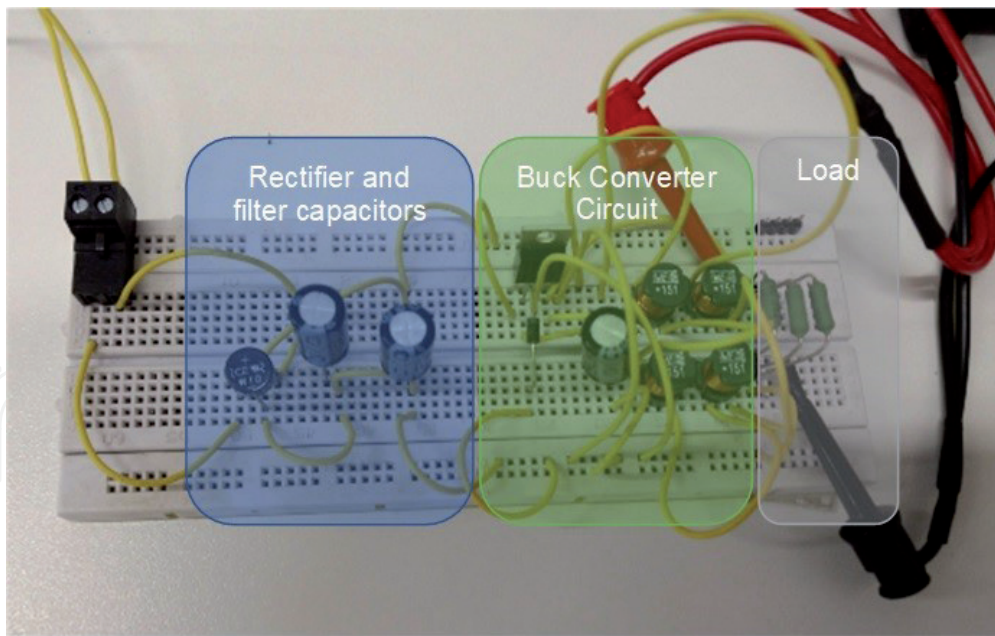


Figure 8. Protoboard assembly of the buck CC-CC converter circuit, including the rectifier and equivalent resistive load.

less than the input voltage and was chosen according to the voltages obtained at the output of the extraction CT in the range of possible currents for the application.

Figure 7 presents the general schematic of the topology and the schematic of the actual circuit implemented with integrated circuit LM2575-5.0.

Figure 8 introduces the protoboard implementation of the buck converter. In this figure, the rectifier with the ripple filtering capacitors, the buck converter itself, and a resistive load equivalent to the estimated load of the application are shown.

4. Wireless interface specifications

There are a large number of wireless communication technologies for the most diverse purposes. Among these, we can cite three well-known: IEEE 802.15.4 known as Zigbee [9], IEEE 802.11 known as Wi-Fi [8], and IEEE 802.15.1 known as Bluetooth [10].

The IEEE 802.15.4 Standard, Zigbee, is an open standard designed exclusively for use in device networks. It is a technology that does not require much processing or power, being suitable for devices with batteries. The standardization is not yet total so that a device with interface said Zigbee would not necessarily be able to communicate with another device with interface. Since the standard is oriented to device networks, “streaming” applications, which require the continuous submission of data at relatively high rates, are not well attended because the maximum baud rate is 250 Kbps. The range can also be a limiting factor for applications based on this standard.

The IEEE 802.11 Standard, Wi-Fi, is best known and commonly used for connecting devices such as notebooks, tablets, and smartphones to Internet routers. The standard uses radio bands in the range of 2, 4, and 5GHz. It is possible to obtain a “Wi-Fi Certified” certification for a device to ensure its full compatibility with the standard and ensure its interoperability with other devices as well as certificates. This standard is quite suitable for “streaming” applications, being used commonly for audio and video streaming applications, much more demanding, in terms of speed, than the transducer proposed in this project. Data transmission rates of 10 Mbps or larger are common. Another positive point is the long range usually obtained with interfaces of this standard, which can reach 100 m or more.

The IEEE 802.15.1 Standard, Bluetooth and Bluetooth Low Energy (BLE), establishes an interface geared to the transmission of data in short distance, 2–10 m. Streaming applications are serviced very well as long as the distance limitation does not adversely affect the application. The data throughput is between 1 and 3 Mbps. Another limiting factor is the limit of seven devices on a Bluetooth network. The Bluetooth standard is well controlled, and every device needs to be certified to use the name.

Thus, considering the general characteristics of these three wireless interface standards, the IEEE 802.11 Standard, Wi-Fi, shows the most indicated, taking into account the general requirements of this application, which are range, greater than 10 m; data transmission rate, in the order of Mbps; and practicality and integration facilitated with the communication network of the plant.

The two most common and known transport layer protocols are transmission control protocol (TCP) and user datagram protocol (UDP). The TCP is one of the main protocols of the Internet protocol set. It enables reliable, orderly, and error-checking packet transmission. The UDP uses a simpler, connectionless communication model. UDP checks the integrity of the data with “checksum” and uses a system of several ports for different functions, both in the target and in the source. There are no handshake dialogs between the source and the destination because there is no established connection. Therefore, there is no guarantee of delivery of packages. Thus, the UDP is suitable for applications where the integrity and correctness of the data are not necessary or can be done in the application itself, avoiding the cost of this processing in the protocol stack. In general, real-time applications that privilege speed use UDP, as it is preferable to lose a package waiting for a delayed package. In the “streaming” data-type applications, the first transport protocol option is UDP.

The application of this device is related to the monitoring of engine condition, and the condition of a motor changes slowly, at least in the parameters of interest. Therefore, if there is a loss of a package compromising a measurement, another measurement can be requested without prejudice to the monitoring. Besides, it is more appropriate for data integrity checking to be done on the target computer, which probably has more processing capacity than the application microcontroller.

The hardware of the prototype Wi-Fi communication interface module consists of the CC3200-LaunchXL card. This board is composed of circuits for the use of external peripherals of the CC3200 microcontroller, circuits for debugging functionalities, and the antenna of the wireless communication system itself.

The CC3200 is a single-chip microcontroller with integrated Wi-Fi connectivity for the Internet of Things applications. Its core consists of an ARM Cortex-M4 processor that allows the implementation of applications with processing and wireless communication interface with a single integrated circuit.

Provisioning on Wi-Fi-type wireless networks is the process of connecting a new Wi-Fi device (called a station) to a Wi-Fi network (called a hotspot). The provisioning process involves loading the station with the network name (called SSID) and the security credentials. The Wi-Fi security standard distinguishes between personal security, for home and business use, and business security, for use in large offices and large networks. In the case of the enterprise security standard, certificates are installed that are used to verify the health of the station and the network by interacting with a secure server managed by the IT department. In the case of the personal security standard, only the use of a password is required.

In the case of CC3200 devices with the SimpleLink application programming interface (API), there are three provisioning methods: SmarConfig, AP mode, and Wi-Fi protected setup (WPS).

The SmarConfig Technology owns the Texas Instruments and consists of a provisioning method for non-peripheral input/output devices (keyboards, mice,

```

476 long wlanConnect()
477 {
478     SIParams_t secParams = {0};
479     long lRetVal = 0;
480
481     secParams.Key = (signed char*)SECURITY_KEY;
482     secParams.KeyLen = strlen(SECURITY_KEY);
483     secParams.Type = SECURITY_TYPE;
484
485     lRetVal = sl_wlanConnect((signed char*)SSID_NAME, strlen(SSID_NAME), 0, &secParams, 0);
486     ASSERT_ON_ERROR(lRetVal);
487
488     // Wait for WLAN Event
489     while(!IS_CONNECTED(g_ulStatus) || !IS_IP_ACQUIRED(g_ulStatus))
490     {
491         // Toggle LEDs to Indicate Connection Progress
492         GPIO_IF_LedOff(MCU_IP_ALLOC_IND);
493         MAP_UtilsDelay(800000);
494         GPIO_IF_LedOn(MCU_IP_ALLOC_IND);
495         MAP_UtilsDelay(800000);
496     }
497
498     return SUCCESS;
499 }
500 }

```

Figure 9.
C code using the SimpleLinkK API to connect to the provisioned Wi-Fi network.

monitors, and CT), as is the case with the application of this project. This method uses an application to broadcast network credentials through a smartphone, tablet, or PC to a Wi-Fi device that has not yet been provisioned.

When the unprovisioned device uses the SmartConfig mode, it enters a special scanning mode, hoping to collect the network information being broadcast by the SmartConfig application on a smartphone, for example. The smartphone needs to be connected to a Wi-Fi network to broadcast its credentials.

The access point (AP) method is the most widespread method for provisioning non-peripheral input/output devices over Wi-Fi networks. In this method, the unprovisioned device starts in access point mode, creating its network with SSIDs and credentials set by the application's manufacturer, so a smartphone or PC can connect directly to the unprovisioned device and configure your provisioning on the desired network. These elements are the provisioning method adopted in the final version of the CT.

The Wi-Fi protected setup (WPS) method is the only industry standard available for provisioning non-peripheral input/output devices. It was introduced by the Wi-Fi Alliance in 2006 and is a safe and easy method of provisioning devices without knowing the SSID of the network or long typing passwords. The default defines two mandatory methods for access points with WPS: using personal identification number (PIN) and using a push-button-connect (PBC).

Once the SSID and the access credentials have been established, the code, shown in **Figure 9**, makes the connection to the chosen network using the SimpleLink application programming interface (API) in C code.

The basic flow of connecting, transmitting, and receiving data with a UDP socket from the SimpleLink application programming interface (API) of the CC3200 microcontroller in C language is presented next to the client and server side.

On the client side, you first create a socket of the IPv4 type and select a UDP connection, as follows:

```

int SockID;
SockID = sl_Socket(SL_AF_INET, SL_SOCKET_DGRAM, 0);

```

In the code above, the first parameter, SL_AF_INET, indicates the selection of an IPv4 socket; the second parameter, SL_SOCKET_DGRAM, selects the UDP protocol; the third parameter, 0, selects the protocol default mode; and the SockID variable

is the handler for the socket that will be used in all subsequent operations. The parameters used above and others are established in the header file “socket. h.”

Because UDP is a connectionless protocol, the client can begin sending data to a specific address without verifying that the device is active or not. The following code is an example of how to do this:

```
#define IP_ADDR      0xc0a80164
#define PORT_NUM    5001

Addr.sin_family     = SL_AF_INET;
Addr.sin_port       = sl_Htons((UINT16) PORT_NUM);
Addr.sin_addr.s_addr = sl_Htonl((UINT32) IP_ADDR);

Status = sl_SendTo(SockID, uBuf.BsdBuf, BUF_SIZE, 0, (SlSockAddr_t *) &Addr,
sizeof(SlSockAddrIn_t));
```

In the code above, IP_ADDR is the IP address in hexadecimal format, PORT_NUM is the port number used, and Addr is a structure that gathers all the necessary information (user-specified information and other standard information) to the operation.

Finally, to close the socket, you use the following function:

```
sl_Close(SockID);
```

On the server side, the creation of the socket is identical to the client side:

```
SockID = sl_Socket(SL_AF_INET, SL_SOCKET_DGRAM, 0);
```

The socket then needs to be bound to the local IP address through the sl_Bind function:

```
#define PORT_NUM    5001

SlSockAddrIn_t LocalAddr;
AddrSize = sizeof(SlSockAddrIn_t);

TestBufLen = BUF_SIZE;

LocalAddr.sin_family     = SL_AF_INET;
LocalAddr.sin_port       = sl_Htons((UINT16) PORT_NUM);
LocalAddr.sin_addr.s_addr = 0;
Status = sl_Bind(SockID, (SlSockAddr_t *) &LocalAddr, AddrSize);
```

From this point, you can try to receive data by the socket of the source specified by Addr, the fifth parameter of sl_RecvFrom:

```
#define BUF_SIZE 1400
SlSockAddrIn_t Addr;
char RecvBuf[BUF_SIZE];

Status = sl_RecvFrom(SockID, RecvBuf, BUF_SIZE, 0, (SlSockAddr_t *) &Addr, (SlSocklen_t*)
&AddrSize );
```

If the “nonblocking” option was not specified, the command is locked until the amount of data specified in BUF_SIZE is received.

To close the socket, use the sl_Close function as before:

```
sl_Close(SockID);
```

5. Assembly of the current transducer

The produced prototype boards are presented in **Figures 10** and **11**.

An enclosure was designed with a more rounded and nicer shape visually. The 3D design can be seen in **Figure 12**.

The enclosure design was executed in Delrin® Resin, conferring resistance and robustness to the prototype. **Figures 13–15** show the prototype in its final enclosure.

Figure 16 below presents the operation flow chart for the prototype device. Once the wireless self-supplied module is installed around the motor cable and there is enough current to drive the power conditioning circuit, a timer starts to count. After a stabilization time, the available power is supplied to the main application modules: microprocessor, wireless interface, and analog-to-digital converter. After that, a Wi-Fi network is created for provisioning, as described in Section 4, or direct connection, if desired. Once the device is connected to the desired Wi-Fi network, it can receive commands from the main software or execute operations according to a setup schedule.

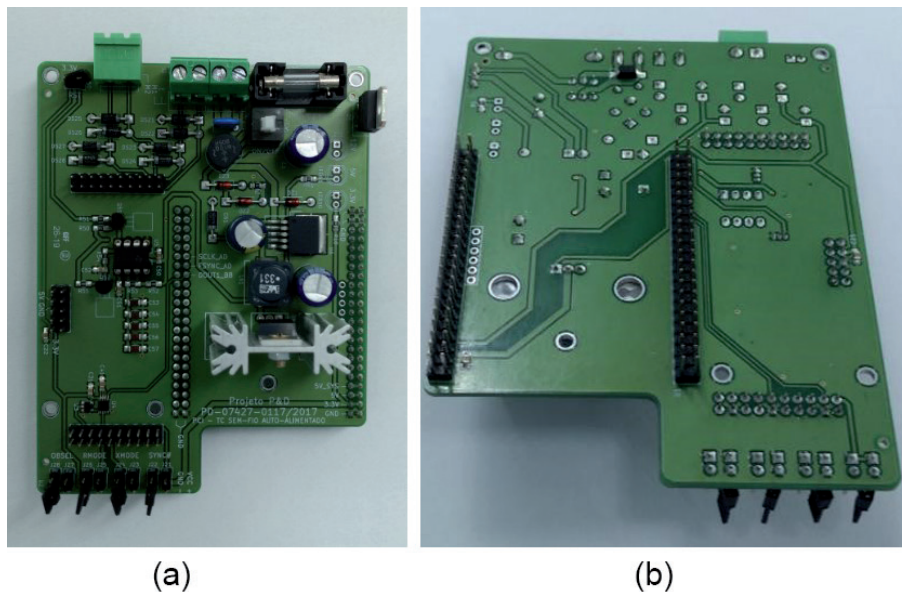


Figure 10.
Device board: (a) top view and (b) bottom view.

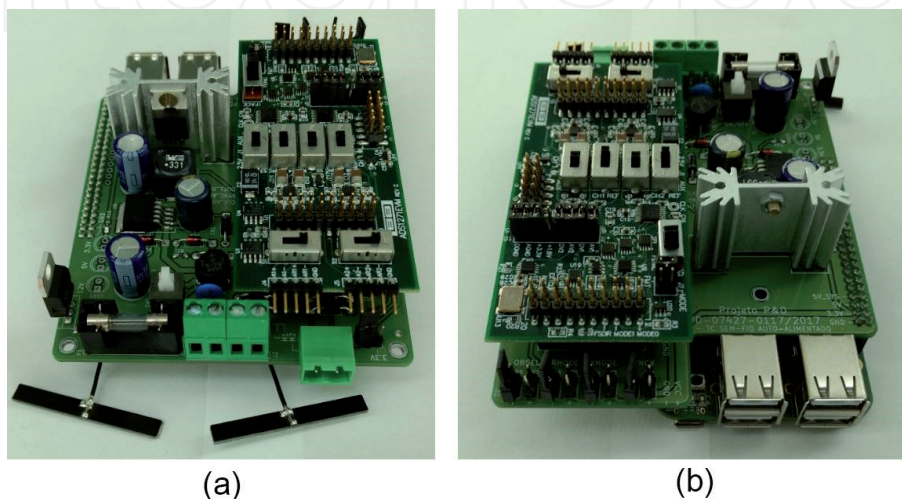


Figure 11.
Board of the device mounted with the SBC and ADS1271-EVM board: (a) front view and (b) rear view.

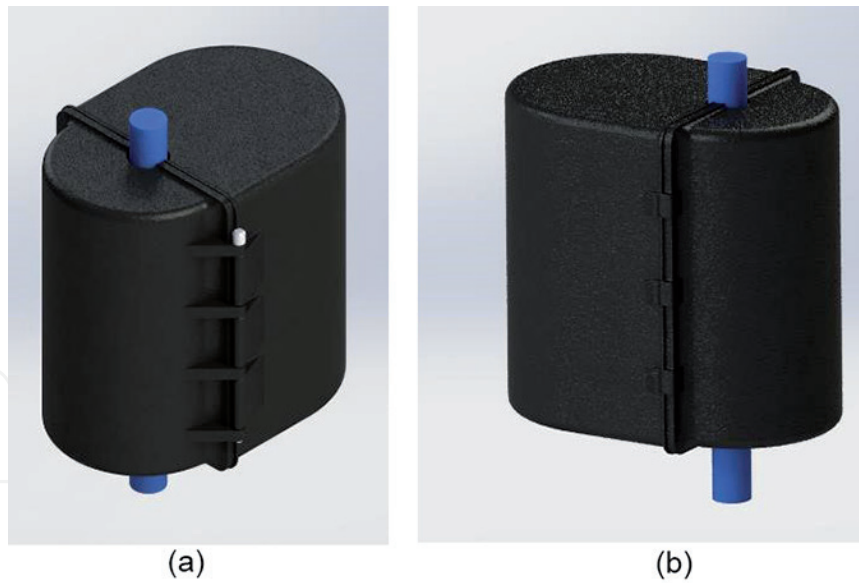


Figure 12.
3D design of the device enclosure.

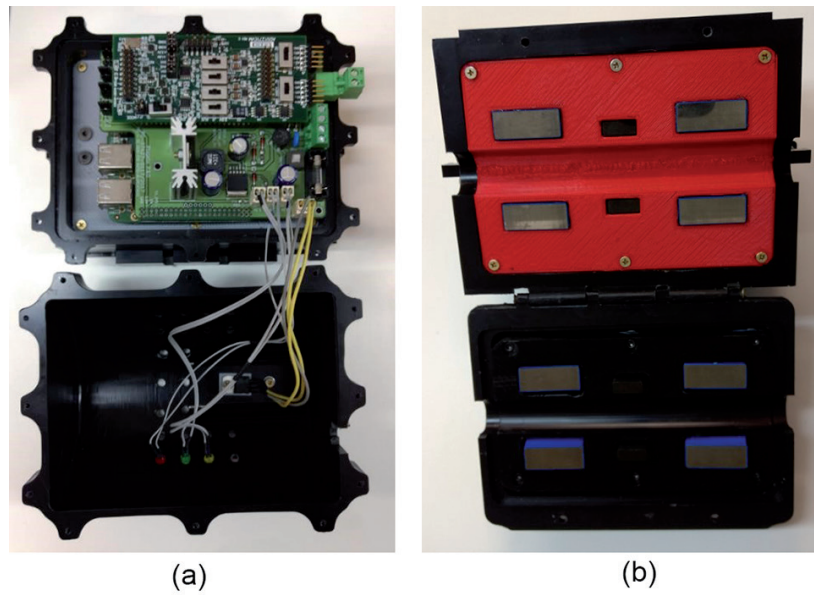


Figure 13.
The open device enclosure exposing (a) the electronics and (b) the CTs for measuring and extracting power.



Figure 14.
Front view of the device.

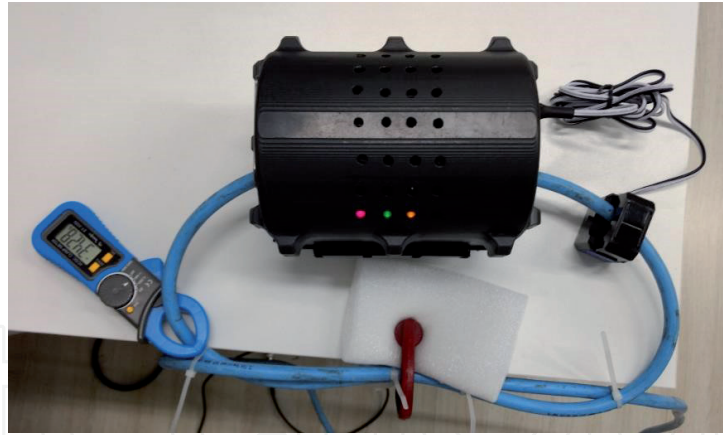


Figure 15.
Device operating in a test setup with 34 A current.

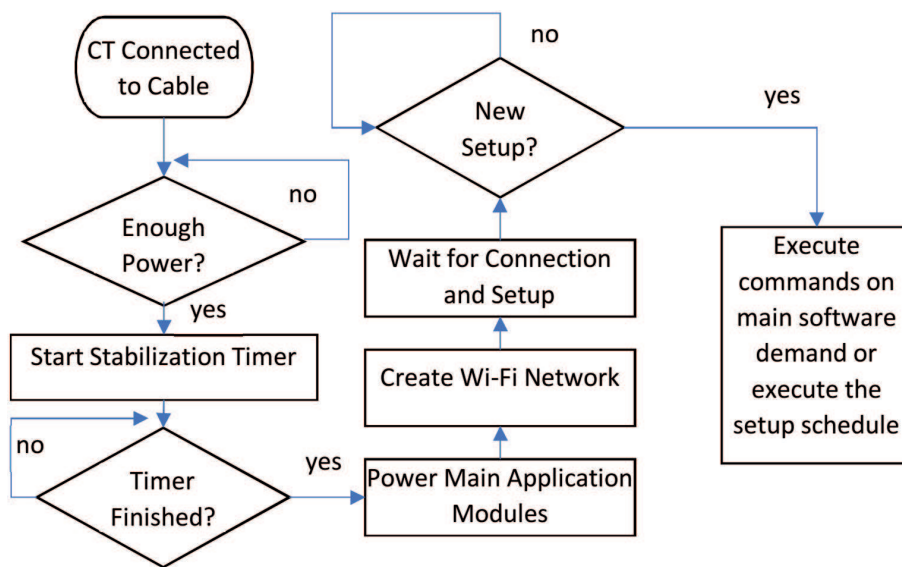


Figure 16.
Operation flowchart for the wireless self-supplied current transducer.

6. Results of tests

6.1 Tests in the laboratory

The objective of these tests was to simulate the actual operating conditions that the device will face when installing on the electric motors in the field. For example, in the case of off-road vehicle (ORV) motors (speed regulator), the prototype must:

- Support the starting condition offered by the “soft-starter” system.
- Work, most of the time, with the current in “no load” (30–60 A).
- Withstand the operating current of the motor (about 162 A), which lasts about 1 min.

Also, for the case of motors without soft starter, the condition of direct starting with currents of the order of six times the nominal current has been tested. For this, a motor of 2.1 A was used, and the cable was passed through one of the phases by the prototype 18 times, producing a motive magnet force of about 36 At in normal

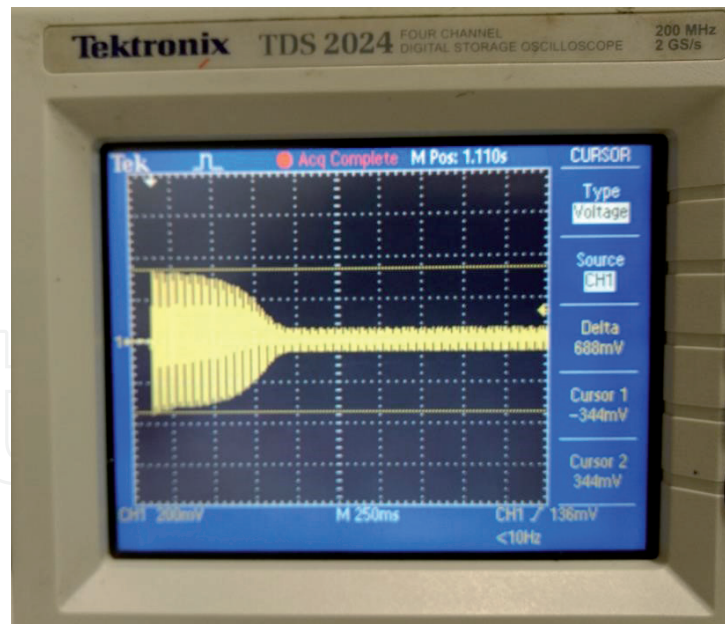


Figure 18.

Engine starting test indicating that the starting current reached about 344 to peak (243 Arms)—the ratio of the current transducer equal to 1 MV/a.

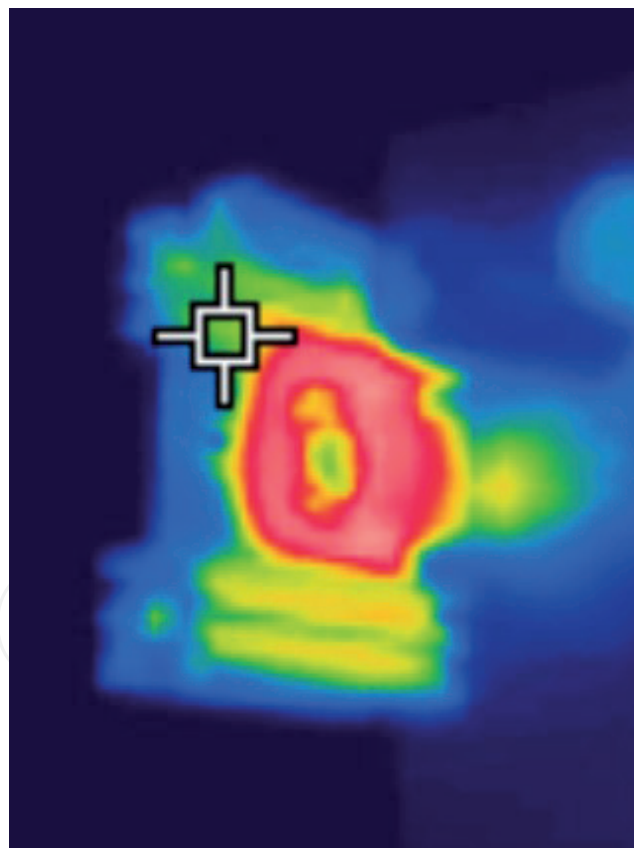


Figure 19.

About 79°C at the hottest point (set operating above the nominal for 4 min).

During the tests, the main subsystem verified was the protection circuit of the buck converter, which prevents the input voltage from being greater than the allowable limit, 40 VDC. In this case, the protection is specified to reap the voltage at about 36 Vcc, keeping the application running and dissipating surplus energy in the protection transistor buffer. The temperature of the transistor/ heat sink assembly was monitored with the extractor operating with a current of 170 A (greater than the operation of about 162 A) over 4 min that is four

times longer than the operating period reported in this condition, as shown in **Figure 19**. The system operated normally, and the maximum temperature in the set reached 79°C.

6.2 Operation at the Pimental hydraulic power plant

Figure 20 presents the device installed and operating in the motor BB-ORV101, at Pimental hydraulic power plant, in Altamira, north of Brazil.

The prototype proved to be stable from a minimum current of about 34 A, as presented in **Figure 21**.

According to field measurements, the BB-ORV motors operate for about 1 min in current slightly higher than the nominal board. This condition was measured and presented in **Figure 22**.



Figure 20.
Device installed at Pimental hydraulic power plant in Brazil.

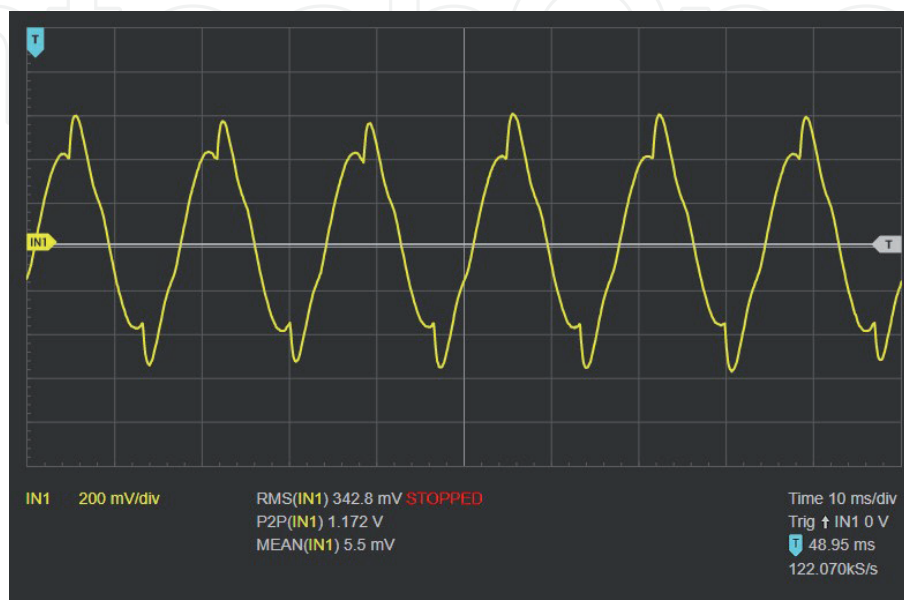


Figure 21.
Waveform presented by the oscilloscope in the current condition of minimum, 34 A.

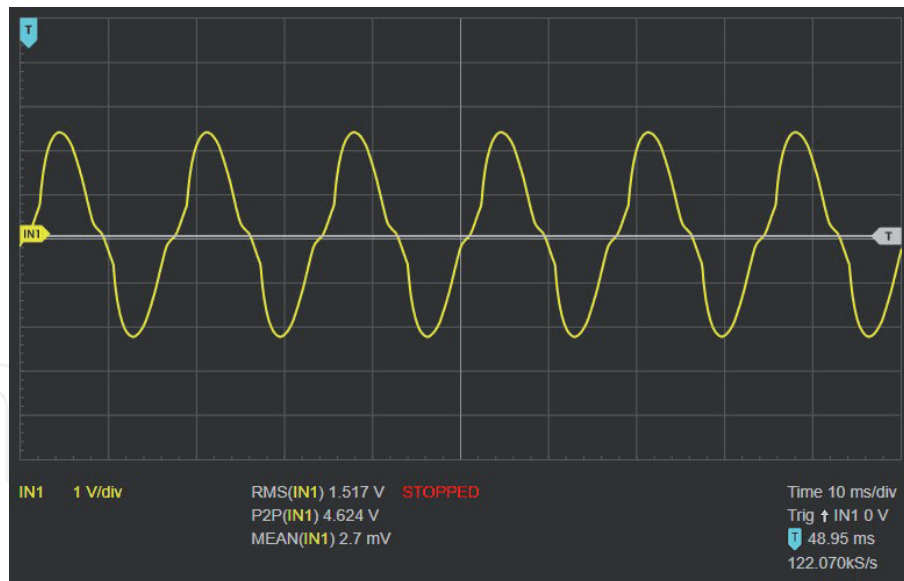


Figure 22.
Waveform presented by the oscilloscope in the current condition near the nominal, 149 A.

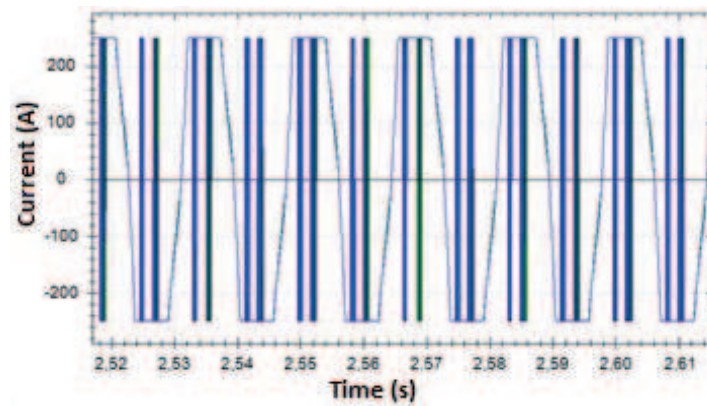


Figure 23.
Saturated and distorted waveform presented by the prototype in the condition of starting current, 602 A.

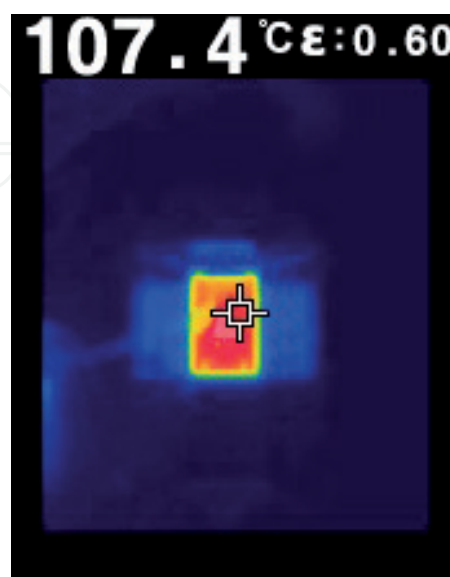


Figure 24.
Thermal image of the transistor/protection sink of the buck converter, in the condition of starting current, 602 A, after about 60 s of operation.

In the field measurements, it was found that in the BB-ORV motors, which have a soft-starter device, the starting condition takes about 4 s and reaches a current of 400 A. To introduce a safety factor, the prototype was subjected to currents of 600 A for more than 60 s. The objective is not that the prototype can measure these currents, as they are far above the nominal CT, which is 200 A but can withstand them without fail. Therefore, it is normal, in this condition, that the prototype displays saturated or distorted currents, as shown in **Figure 23**. **Figure 24** shows the thermal image of the transistor/protection sink of the buck converter, in the condition of starting current, 602 A, after about 60 s of operation.

6.3 Considerations about the power harvesting capability of the prototype

The power harvesting capability of the prototype reaches 2.5 W in the condition of a minimum current of 34 A in the measured cable. This power suffices to drive a single-board computer based on an ARM microprocessor with 64 bit architecture, 1 GHz clock, 512 Mb RAM, Linux operating system, and many peripherals. Such a system is able to perform many digital signal processing (DSP) techniques in the electric current signals acquired from the monitored electric motor, for motor monitoring applications do not require a real-time processing, since a few signals a day suffice for a condition diagnostics of the slow developing faults that can be monitored by the current spectral analysis technique.

7. Conclusions

This chapter aims to show the development and implementation of an innovative current transducer inserted in the context exposed above, i.e., dynamic current measurement (waveform) or its RMS value, for the purpose of monitoring the energy and/or monitoring the condition of assets; wireless interface with remote viewing and/or recording device, self-powered by the magnetic field of the current measure, without connection to the electrical system through external sources and power cords; and ability to synchronize with other gauges or use a real-time base, allowing the correlation of the measurements of various transducers in the same time base.

The main objective of this chapter was to present the development of a current transducer with wireless data transmission self-supplied by the magnetic field of the transduced current. The proposed measuring device involves the cable, whose current is intended to be measured, extracting power from the magnetic field around the conductor to feed the current transducer itself and the data flow generator circuit of the measured current (“streaming”) through a wireless transmission protocol. The measured current can be viewed on a handheld device such as a “smartphone” or data collector, for example. The extracted signal was used to monitor the condition of the cooling system motors of the Pimental hydraulic power plant through the analysis of the electrical signature analysis.

The main advantages of the proposed system are:

- Ease of installation: the device involves the cable whose current is to be measured.
- Easy access to data: wireless and remote interface with data collectors or “smartphones.”

- Nonintrusive: the only interface with the system to be measured is the magnetic field, and there will be no sources or cables interfering with the electrical panels of the plant.
- Record of the data in the “cloud” if desirable.
- Ease of implementation of energy monitoring and condition-based maintenance applications.

Acknowledgements

The academic authors would like to express their thanks to the ANEEL Research and Development, CNPq, CAPES, FINEP, and FAPEMIG for supporting this work.

Author details

Erik Leandro Bonaldi¹, Levy Ely de Lacerda de Oliveira¹, Germano Lambert-Torres^{1*}, Luiz Eduardo Borges da Silva² and Vitor Almeida Bernardes³

1 Itajuba Federal University, Brazil

2 Gnarus Institute, Brazil

3 Norte Energia, Altamira, Brazil

*Address all correspondence to: germanoltorres@gmail.com

IntechOpen

© 2020 The Author(s). Licensee IntechOpen. Distributed under the terms of the Creative Commons Attribution - NonCommercial 4.0 License (<https://creativecommons.org/licenses/by-nc/4.0/>), which permits use, distribution and reproduction for non-commercial purposes, provided the original is properly cited. 

References

- [1] Haj-Yahya J, Mendelson A, Ben Asher Y, Chattopadhyay A. Power modeling at high-performance computing processors. In: Haj-Yahya J, Mendelson A, Ben Asher Y, Chattopadhyay A, editors. *Energy Efficient High Performance Processors*. 1st ed. Singapore: Springer Singapore; 2018. pp. 73-105. DOI: 10.1007/978-981-10-8554-3_3
- [2] Salman T, Networking Protocols JR. Standards for Internet of Things. In: Geng H, editor. *Internet of Things and Data Analytics Handbook*. 1st ed. Indianapolis (IN): John Wiley & Sons; 2017. pp. 215-238. DOI: 10.1002/9781119173601.ch13
- [3] Chou T. *Precision: Principles, Practices and Solutions for the Internet of Things*. 1st ed. Birmingham(UK): Lulu.com; 2016. 312p
- [4] Kellmerit D, Obodovski D. *The Silent Intelligence: The Internet of Things*. 1st ed. DnD Ventures: Warwick (NY); 2013. 156p
- [5] Lea P. *Internet of Things for Architects: Architecting IoT Solutions by Implementing Sensors, Communication Infrastructure, Edge Computing, Analytics, and Security*. 1st ed. Morrisville (NC): Packt Publishing; 2018. 524p
- [6] Gilchrist A. *Industry 4.0: The Industrial Internet of Things*. 1st ed. New York City: Apress; 2016. 250p
- [7] Ustundag A, Cevikcan E. *Industry 4.0: Managing the Digital Transformation*. 1st ed. Chan (Switzerland): Springer International Publishing; 2016. 286p. DOI: 10.1007/978-3-319-57870-5
- [8] IEEE Standard. IEEE 802.11. 2019. Available from: <https://ieeexplore.ieee.org/browse/standards/get-program/page/series?id=68>
- [9] IEEE Standard. IEEE 802.15.4. 2018. Available from: <https://ieeexplore.ieee.org/document/8410916>
- [10] IEEE Standard. IEEE 802.15.1. 2005. Available from: <https://ieeexplore.ieee.org/document/1490827>